Environmental Toxicology and Pharmacology 42 (2016) 30–37

Contents lists available at ScienceDirect

Environmental Toxicology and Pharmacology

journal homepage: www.elsevier.com/locate/etap

# Molecular and biochemical evidence on the protection of cardiomyocytes from phosphine-induced oxidative stress, mitochondrial dysfunction and apoptosis by acetyl-L-carnitine

Amir Baghaei[a,b], Reza Solgi[c,d], Abbas Jafari[e], Amir Hossein Abdolghaffari[f], Alireza Golaghaei[b], Mohammad Hossein Asghari[b], Maryam Baeeri[b], Seyed Nasser Ostad[b], Mohammad Sharifzadeh[b], Mohammad Abdollahi[b,*]

[a] Department of Toxicology and Pharmacology, Faculty of Pharmacy, Alborz University of Medical Sciences, Karaj, Iran
[b] Department of Toxicology and Pharmacology, Faculty of Pharmacy; and Pharmaceutical Sciences Research Center; and Poisoning & Toxicology Research Center; and Endocrinology & Metabolism Research Center, Endocrinology and Metabolism Clinical Sciences Institute, Tehran University of Medical Sciences, Tehran 1417614411, Iran
[c] Metabolic Disorders Research Center, Golestan University of Medical Sciences, Gorgan, Iran
[d] Department of Pharmacology, Faculty of Medicine, Golestan University of Medical Sciences, Gorgan, Iran
[e] Department of Pharmacology and Toxicology, Faculty of Pharmacy, Urmia University of Medical Sciences, Urmia, Iran
[f] Medicinal Plants Research Center, Institute of Medicinal Plants, ACECR, Karaj, Iran

ARTICLE INFO

*Article history:*
Received 14 July 2015
Received in revised form
22 December 2015
Accepted 26 December 2015
Available online 2 January 2016

*Keywords:*
Acetyl-L-carnitine
Cytochrome c oxidase
Oxidative stress
Phosphine

ABSTRACT

The aim of the present study was to investigate the efficacy of acetyl-L-carnitine (ALCAR) on pathologic changes of mitochondrial respiratory chain activity, ATP production, oxidative stress, and cellular apoptosis/necrosis induced by aluminum phosphide (AlP) poisoning. The study groups included: the Sham that received almond oil only; the AlP that received oral $LD_{50}$ dose of aluminum; the AC-100, AC-200, and AC-300 which received concurrent oral $LD_{50}$ dose of AlP and single 100, 200, and 300 mg/kg of ALCAR by intraperitoneal injection. After 24 h, the rats were sacrificed; the heart and blood sample were taken for measurement of biochemical and mitochondrial factors. The results specified that ALCAR significantly attenuated the oxidative stress (elevated ROS and plasma iron levels) caused by AlP poisoning. ALCAR also increased the activity of cytochrome oxidase, which in turn amplified ATP production. Furthermore, flow cytometric assays and caspase activity indicated that ALCAR prohibited AlP-induced apoptosis in cardiomyocytes.



## 1. Introduction

Pesticide poisoning is accountable for annually 300,000 casualties around the world. Organophosphorus and metal phosphides (aluminum and zinc phosphide) keep the highest rate in this regard. Aluminum phosphide (AlP) is widely used as an effective insecticide and rodenticide (in the shape of tablets, pellets, etc.) to protect stored grains (Mehrpour et al., 2012). Phosphine gas ($PH_3$) generated from AlP combines with humidity in the air and plays the pesticide role. $PH_3$ is colorless and odorless (though impurities in tablets cause garlic smell while sublimated). Moreover, phosphine density is approximately equal to the air (1.17 times) that allows it to spread easily. $PH_3$ is extremely toxic to aerobic and metabolically active organisms (Nath et al., 2011). For instance, ingestion of as small as 500 mg of AlP would potentially result in death for adults. The main clinically proven cause of death is severe and refractory hypotension subsequent to heart failure (Siwach et al., 1998). To date, there has been a little agreement on the exact site or mechanism of action and it has yet to be determined. Nevertheless, there are two most accepted mechanisms for explanation of $PH_3$ toxicity; the first is uncoupling of mitochondrial electron transport chain through inhibition of mitochondrial complex IV (cytochrome C oxidase) which leads to decreased ATP production and cellular energy level. The second is induction of oxidative stress via inhibition of antioxidant enzymes (superoxide dismutase, catalase and peroxidase) and release of iron from transferrin that causes iron-catalyzed reactive oxygen species (ROS) production by Fenton's and Haber–Weiss reactions, resultant

* Corresponding author.
*E-mail address:* Mohammad@TUMS.Ac.Ir (M. Abdollahi).

http://dx.doi.org/10.1016/j.etap.2015.12.019
1382-6689/

damage to cellular macromolecules and cell death (Anand et al., 2011). Despite numerous studies to find an effective treatment for AlP poisoning and proposing a variety of substances (including trimetazidine, Mg-carrying nanoparticles, IMOD™, Vasopressin plus milrinone, Iron sucrose, triiodothyronine, etc.) there is still no cure for it (Abdolghaffari et al., 2015; Baeeri et al., 2013; Baghaei et al., 2014; Duenas et al., 1999; Jafari et al., 2015; Solgi et al., 2015).

As mentioned above, probable mechanisms of $PH_3$ toxicity are suppression of mitochondrial respiration, inhibition of antioxidant enzymes and enhancement of free iron-dependent reactive oxygen species (ROS) production. ALCAR is a natural occurring substance which acts by stimulating energy metabolism. It is intimately involved in transporting long-chain fatty acids across the mitochondrial inner membrane for oxidative phosphorylation and ATP production. Previous studies have indicated that ALCAR is capable of increasing both activity and expression of mitochondrial complex IV in rat cardiomyocytes and mouse hepatocytes (Cha and Sachan, 1995; Cui et al., 2003). Furthermore, it is revealed that ALCAR modulates antioxidant enzymes in pathophysiological conditions (Loots et al., 2004). In addition, ALCAR has shown remarkable ferrous metal ion chelating activity that is comparable to EDTA (Gulcin, 2006). Moreover, it has been proven by several in vitro studies that ALCAR is able to block mitochondrial pathway apoptosis, which plays a crucial role in cardiomyocytes death by AlP intoxication (Pillich et al., 2005). Based on given mechanisms, this project will focus on potential protective mechanisms of ALCAR in acute AlP poisoning.

## 2. Materials and methods

### 2.1. Chemicals

AlP was purchased from Samiran Pesticide Formulating Co. (Tehran, Iran). ALCAR (99% purity) was purchased from Sigma Aldrich Chemie (Munich, Germany). The mitochondria isolation kit was obtained from Bio-Chain Ins. (Newark, New Jersey, USA). Annexin V-FITC/PI was obtained from Beijing Biosea Biotechnology Co, Ltd (Beijing, China). Adenosine diphosphate (ADP) sodium salt, adenosine triphosphate (ATP) disodium salt, tetrabutylammoniumhydroxide (TBAHS), methanol (HPLC grade), column (SUPELCOSIL™ LC-18-T) from Supelco (Antrim, UK), acetic acid, $FeCl_3{\cdot}6H_2O$, sodium sulfate, trichloroacetic acid (TCA), potassium dihydrogen phosphate anhydrous ($KH_2PO_4$, analytical grade), 2,4,6-tripyridyl-s-triazine (TPTZ), 2-thiobarbituric acid (TBA), rotenone, 2,6-dichloroindophenol (DCIP), antimycin A, collagenase and other chemicals were of the highest purity available and were purchased from Sigma Aldrich Chemie (Munich, Germany).

### 2.2. Animals

Male Wistar rats weighing between 200 and 220 g were used in the study. Animals were housed singly in standard cages in a controlled room temperature and humidity and light–dark cycle. Animals were fed a normal laboratory diet. Rats were deprived of food for 12 h prior to experiments, but were allowed free access to tap water. Experiments followed a protocol that was approved by the institutional review board and the ethics committee with code number 91-03-33-19006.

### 2.3. Experimental design

Forty-five rats were randomly assigned to five groups of each nine animals. AlP was dispersed in almond oil and administered by gavage. ALCAR was dissolved in sterile normal saline (NS) and administered intraperitoneally (IP) at doses of 100, 200 and 300 mg/kg. Doses of ALCAR were picked from previous studies (Jia et al., 2014; Paradies et al., 1992; Patel et al., 2012). Pentobarbital was used for induction of anesthesia.

Animals which received almond oil only was named as Sham; aluminum phosphide as AlP; AlP + ALCAR (100 mg/kg) as AC-100; AlP + ALCAR (200 mg/kg) as AC-200; AlP + ALCAR (300 mg/kg) as AC-300.

Prior to the beginning of experiment, animals were fasted for 12 h. AlP was gavaged to all animals except for Sham group. All treatments were performed after 30 min to all groups except for Sham and AlP group. At 24 h post treatments, the animals were decapitated and the heart and blood were removed. Plasma was separated from blood and frozen at −20 °C. The heart was rinsed in ice-cold saline. Six heart samples of each group were frozen in liquid nitrogen and stored at −80 °C for further mitochondrial and biochemical studies and three samples were immediately used for flow cytometric analysis.

### 2.4. Determination of AlP $LD_{50}$

Karber's method was used to determine the $LD_{50}$ of obtained AlP powder. According to the method, four groups of each containing four rats were selected and AlP was administered at doses of 8, 10, 12, and 14 mg/kg. The calculated $LD_{50}$ based on the number of dead animals after 24 h was approximately 12 mg/kg (Baghaei et al., 2014).

### 2.5. Mitochondrial isolation and assay for mitochondrial function

According to Sigma mitochondrial isolation kit instructions, 100 mg (50–200 mg) of fresh heart tissue, which was collected 24 h after treatment was used. Through the 15 steps of tissue treatment (involving three-step centrifugation), tissue mitochondria were isolated. Isolated mitochondrial samples were immediately assayed for protein content and refrigerated for mitochondrial complexes activity assays. All procedures were done under the temperature 0–4 °C.

### 2.6. Measurement of complex I (NADH dehydrogenase) activity

The basis of this test is measuring the oxidation of NADH to NAD at 340 nm with 380 nm as the reference wavelength at 37 °C. The assay of complex I (NADH dehydrogenase) was performed on 25 mM $KPO_4$ buffer (pH 7.2) containing mitochondrial protein (6 mg), 5 mM $MgCl_2$, 1 mM KCN, 1 mg/ml BSA, and 150 μM NADH; the reaction was initiated by the addition of coenzyme Q (50 μM). In this reaction, ubiquinone is the final electron acceptor. The difference in activity with and without rotenone at a fully saturating level of 5 mM is calculated to differentiate complex I activity from that of the rotenone-insensitive NADH, ubiquinone oxidoreductase (Janssen et al., 2007).

### 2.7. Measurement of complex II (succinate dehydrogenase) activity

The enzymatic activity of Complex II was determined spectrophotometrically by the rate of succinate-driven, co-enzyme Q2-related reduction of dichlorophenolindophenol (DCPIP). Briefly, mitochondria were incubated in phosphate buffer (pH 7.4) containing 40 μM DCPIP, 1 mM KCN, 10 μM rotenone, and 50 μM co-enzyme Q2. The rate of DCPIP reduction to DCPIPH2 was determined at 600 nM. At the end of each run thenoyltrifluoroacetone (1 mM) was added and the residual TTFA insensitive rate was subtracted (Tompkins et al., 2006).

### 2.8. Measurement of complex IV (cytochrome-c oxidase) activity

Method of Smith was used to assay cytochrome oxidase kinetics. Briefly, the ferrocytochrome c oxidation rate was measured by subsequent declines in absorbance at 550 nm. The assays were performed by using 50 mm PO4-2 (pH 7.0), 2% lauryl maltoside, and 1 μg of mitochondrial protein. For the initiation of the reaction, ferrocytochrome c was added at a concentration of 40 mm. Specific activity was determined from mean values of three to four measurements using 21.1 $mM^{-1}$ $cm^{-1}$ as the extinction coefficient of ferrocytochrome c at 550 nm (Smith, 1955).

### 2.9. Measurement of cardiac ADP and ATP

Isolated hearts were minced and homogenized in 1 ml of 6% ice-cold TCA. The homogenate was centrifuged at 12,000 × *g* for 10 min at 4 °C. The supernatant was neutralized by 4 M KOH to pH 6.5, filtered through a Millipore filter (pore size 0.45 μm), and used to determine the quantity of ATP and ADP (μg/ml per mg of tissue) using Ion-pair HPLC (Baeeri et al., 2013).

### 2.10. Measurement of free plasma iron

Performed by the spectrophotometric method of Nilsson et al. Briefly 2 ml of ventricular blood was taken after the decapitation of each animal, transferred into heparinated tubes and centrifuged at 1000 × *g* for 10 min to separate plasma from cells. Plasma samples, then filtered through Millipore filters. Two 75 μl portions of filtered plasma were drawn and BPS was added to one of them. After 15 min, the absorption was seen at 535 nm and free plasma iron concentration was calculated from the difference of absorption (Nilsson et al., 2002).

### 2.11. Measurement of ROS

ROS generation in heart tissue was measured by dichlorofluorescein (DCF) probe using LeBel and Bondy method. The DCF assay was performed within 1 h of tissue sampling. Briefly, fresh 2′,7′-dichlorofluorescin acetate (DCFH-DA) stock solution was made by dissolving it in 1.25 mM methanol and kept in a dark room at 0 °C. 50 μl of homogenate were added to a cuvette containing 3 μl of 0.1 M phosphate buffer (pH 7.4), and 12 μl of 1.25 mM DCFH-DA (total volume 5 0.3 ml). DCFH-DA was dissolved in methanol to facilitate the penetration into cells. The mixture was incubated for 15 min at 37 °C to allow the DCFH-DA probe to cross any membranes and for nonspecific esterases to cleave to diacetate groups. DCF formation was determined by a spectrofluorometer at excitation wavelength of 488 nm and emission wavelength of 525 nm at 37 °C. Measurements were made every 15 min for 60 min, and linear DCF production rate was determined relative to the amount of protein added to the cuvette. The results are showed as nanomole DCF formed per minute per milligram protein (Brubacher and Bols, 2001).

### 2.12. Measurement of superoxide dismutase (SOD) activity

The activity of SOD was determined according to the method of Minami and Yoshikawa. In brief, tissue homogenates were put for 2 min in 0.154 M NaCl solution (1:50, W/V) at 4 °C. Then 5 ml of mixture was shaken with ethanol and chloroform and centrifuged for 60 min at 15,000 × *g*. The supernatant was used as the stopper of pyrogallol auto-oxidation reaction and the difference between auto-oxidation of pyrogallol alone and in the presence of cytosolic fraction determined enzymatic activity (Minami and Yoshikawa, 1979).

### 2.13. Measurement of catalase (CAT) activity

For determination of tissue catalase activity, method of Slaughter and O'brien was used. The basis of this method is a colorimetric reaction in which the reaction between color producing reagent (reagent 1) and reaction-initiating reagent (reagent 2) produces hydrogen peroxide that in reaction with Trinder reagent (AP and DHBS) by the enzyme horse radish peroxidase generates a color with 505 nm absorbance. Presence of tissue catalase, inhibits the color development. One unit of catalase activity was defined as the amount of enzyme activity that causes 50% inhibition of color development (Slaughter and O'Brien, 2000).

### 2.14. Measurement of cellular apoptosis by active caspase-3

The test was carried out by using "Sigma Caspase 3 Assay Kit". The Caspase 3 Colorimetric Assay Kit is based on the hydrolysis of acetyl-Asp-Glu-Val-Asp p-nitroanilide (Ac-DEVD-pNA) by caspase 3, resulting in the release of the p-nitroaniline (pNA) moiety. The pNA is detected at 405 nm (εmM = 10.5). The concentration of the pNA released from the substrate is calculated from either the absorbance values at 405 nm.

### 2.15. Measurement of cellular apoptosis by active caspase-9

"Abcam Caspase-9 Colorimetric Assay Kit" was used to determine the amount of active caspase-9. Activation of ICE-family proteases/caspases initiates apoptosis in mammalian cells. The assay is based on spectrophotometric detection of the chromophore p-nitroaniline (pNA) after cleavage from the labeled substrate LEHD-pNA. The PNA light emission can be quantified using a Microtiter plate reader at 405 nm.

### 2.16. Determination of cell viability by flow cytometry

As mentioned above, three heart samples of each group were used for the flow cytometric assay. Left ventricles were rapidly removed and underwent cardiomyocyte isolation by collagenase digestion according to Schluter and Schreiber method (Schluter and Schreiber, 2005). Afterward, the cells were washed with phosphate-buffered saline (PBS) at room temperature and stained with annexin V-FITC and propidium iodide (PI). The stained cells were incubated in binding buffer and analyzed cell death by flow cytometry (Apogee, UK). Data were provided and analyzed with the apogee histogram software. Density plots of flow cytometry are included; the percentage of viable cells (lower left quadrant; annexin $V^-$; $PI^-$), the percentage of apoptotic cells (lower right quadrant; annexin $V^+$; $PI^-$), late apoptotic cells (upper right quadrant; annexin $V^+$; $PI^+$), and necrotized cells (upper left quadrant; annexin $V^-$; $PI^+$) (Jafari et al., 2015).

### 2.17. Statistical analysis

The StatsDirect version 3.0.150 was used for the analyses. Data are expressed as mean ± standard error of the mean (SEM). One-way analysis of variance (ANOVA) followed by Tukey's post hoc for multiple comparisons was used. *P* values less than 0.05 were considered statistically significant.

## 3. Results

### 3.1. Activity of mitochondrial complexes

No significant change in complex I activity was observed between groups ($P > 0.05$). As well, levels of succinate dehydrogenase activity were comparable between all groups and neither

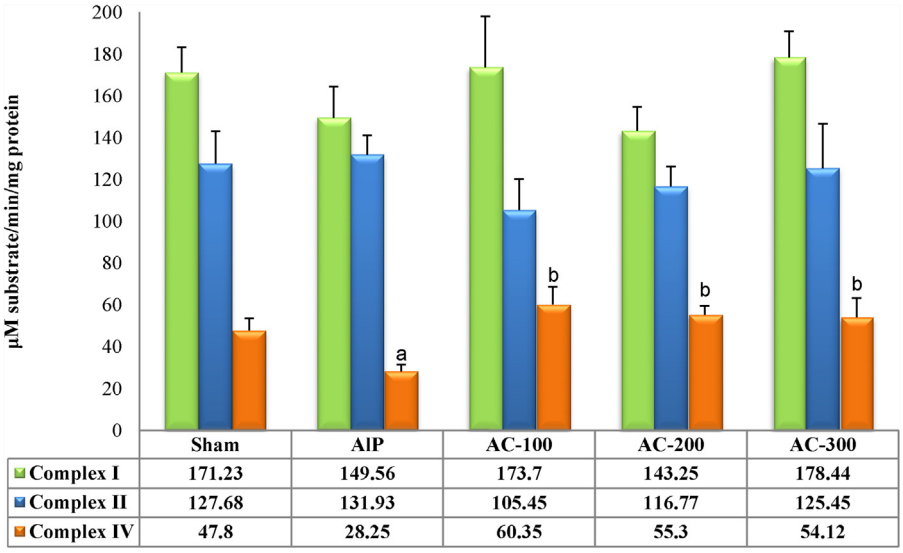


| | Sham | AlP | AC-100 | AC-200 | AC-300 |
|---|---|---|---|---|---|
| Complex I | 171.23 | 149.56 | 173.7 | 143.25 | 178.44 |
| Complex II | 127.68 | 131.93 | 105.45 | 116.77 | 125.45 |
| Complex IV | 47.8 | 28.25 | 60.35 | 55.3 | 54.12 |

**Fig. 1.** Activity of mitochondrial complexes after treatments. Values are mean ± SEM. [a]$P < 0.05$ vs the Sham group; [b]$P < 0.05$ vs the AlP group. Sham: no interventions; AlP: aluminum phosphide at dose of $LD_{50}$; AC-100: acetyl-L-carnitine at dose of 100 mg/kg; AC-200: acetyl-L-carnitine at dose of 200 mg/kg; AC-300: acetyl-L-carnitine at dose of 300 mg/kg.

exposure to AlP nor the administration of ALCAR changed the activity of mitochondrial complex II as compared to the Sham group ($P > 0.05$). Whereas, AlP led to a significant decrease in cytochrome-c oxidase activity when compared to Sham ($P < 0.05$) while the administration of ALCAR at all doses caused significant rise in complex IV activity ($P < 0.05$) and activity levels in all three groups were near to that of the Sham group ($P < 0.05$, Fig. 1).

### 3.2. Cardiac ADP/ATP ratio

The ADP/ATP ratio was higher in the AlP group compared to the Sham ($P = 0.000$). The ADP/ATP ratio in all ALCAR-treated groups was lower than that of the AlPs ($P < 0.01$). Whereas, a higher ADP to ATP ratio was observed in ALCAR treated groups as compared to the Sham ($P < 0.05$, Fig. 2).

### 3.3. Reactive oxygen species (ROS)

The ROS value was significantly higher in the AlP group compared to the Sham ($P < 0.01$). Treatment by ALCAR led to remarkable decline in ROS as compared to Sham ($P < 0.05$). Though ROS levels were significantly higher than the Sham in all ALCAR treated groups ($P < 0.05$). Among ALCAR groups, AC-300 showed lower, but non-significant ROS value ($P > 0.05$, Table 1).

### 3.4. Free plasma iron

Acute oral exposure to AlP leaded to significant rise in plasma iron as compared to the Sham group ($P < 0.001$). Administration of ALCAR at all doses caused a remarkable decline in free plasma iron in comparison with the AlP group ($P < 0.001$). Moreover, plasma iron

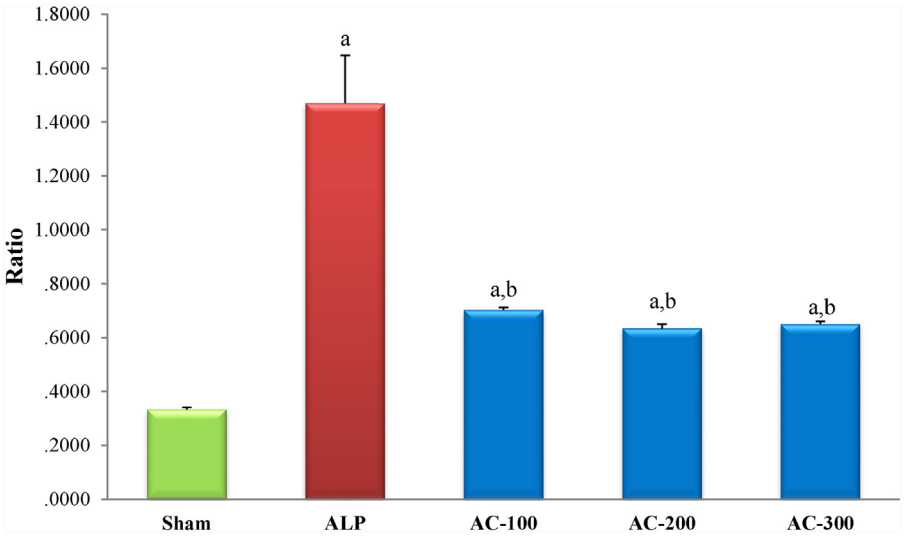


**Fig. 2.** ADP/ATP ratio in heart tissue. Values are mean ± SEM. [a]$P < 0.05$ vs the Sham group; [b]$P < 0.05$ vs the AlP group. Sham: no interventions; AlP: aluminum phosphide at dose of $LD_{50}$; AC-100: acetyl-L-carnitine at dose of 100 mg/kg; AC-200: acetyl-L-carnitine at dose of 200 mg/kg; AC-300: acetyl-L-carnitine at dose of 300 mg/kg.

**Table 1**
Levels of different biochemical parameters after treatment.

| Groups | ROS* (U/mg protein) | Free plasma iron (μM) | CAT# activity (U/mg protein) | SOD+ activity (U/mg protein) |
|---|---|---|---|---|
| Sham | 18.39 ± 4.45 | 1.58 ± 0.15 | 28.11 ± 3.12 | 0.31 ± 0.03 |
| AlP | 88.25 ± 3.65[a] | 6.43 ± 0.37[a] | 17.14 ± 1.09[a] | 0.39 ± 0.13 |
| AC-100 | 46.54 ± 6.30[a,b] | 2.76 ± 0.17[a,b] | 31.99 ± 3.04[a,b] | 0.40 ± 0.08 |
| AC-200 | 55.59 ± 5.99[a,b] | 2.50 ± 0.13[a,b] | 25.86 ± 4.60[b] | 0.38 ± 0.07 |
| AC-300 | 45.36 ± 8.26[a,b] | 2.82 ± 0.19[a,b] | 29.09 ± 5.63[b] | 0.36 ± 0.01 |

Values are mean ± SEM. Sham: no interventions; AlP: aluminum phosphide at dose of $LD_{50}$; AC-100: acetyl-L-carnitine at dose of 100 mg/kg; AC-200: acetyl-L-carnitine at dose of 200 mg/kg; AC-300: acetyl-L-carnitine at dose of 300 mg/kg.
[a] $P < 0.05$ vs the Sham group.
[b] $P < 0.05$ vs the AlP group.
* ROS: reactive oxygen species.
# CAT: catalase.
+ SOD: superoxide dismutase.

levels in all ALCAR groups were comparable to the Sham ($P > 0.05$, Table 1).

### 3.5. Antioxidant enzymes

No significant changes were observed between groups in the case of SOD activity ($P > 0.05$). A significant lower CAT level was seen in the AlP group as compared to the Sham ($P < 0.05$). The level of CAT in AC-100 and AC-300 groups was near to that of the Sham and both were significantly higher than the AlP ($P < 0.05$). CAT level in AC-200 group showed no statistical difference compared to the Sham and the AlP groups ($P > 0.05$, Table 1).

### 3.6. Cell viability

A significant difference in viable cells was seen among AlP and Sham group ($P = 0.001$). Cell viability was significantly raised in all ALCAR groups when compared to AlP ($P < 0.05$). Cell viability in AC-100 and AC-300 was near to that of the Sham group ($P > 0.05$). Fraction of early and late apoptotic cells was also significantly

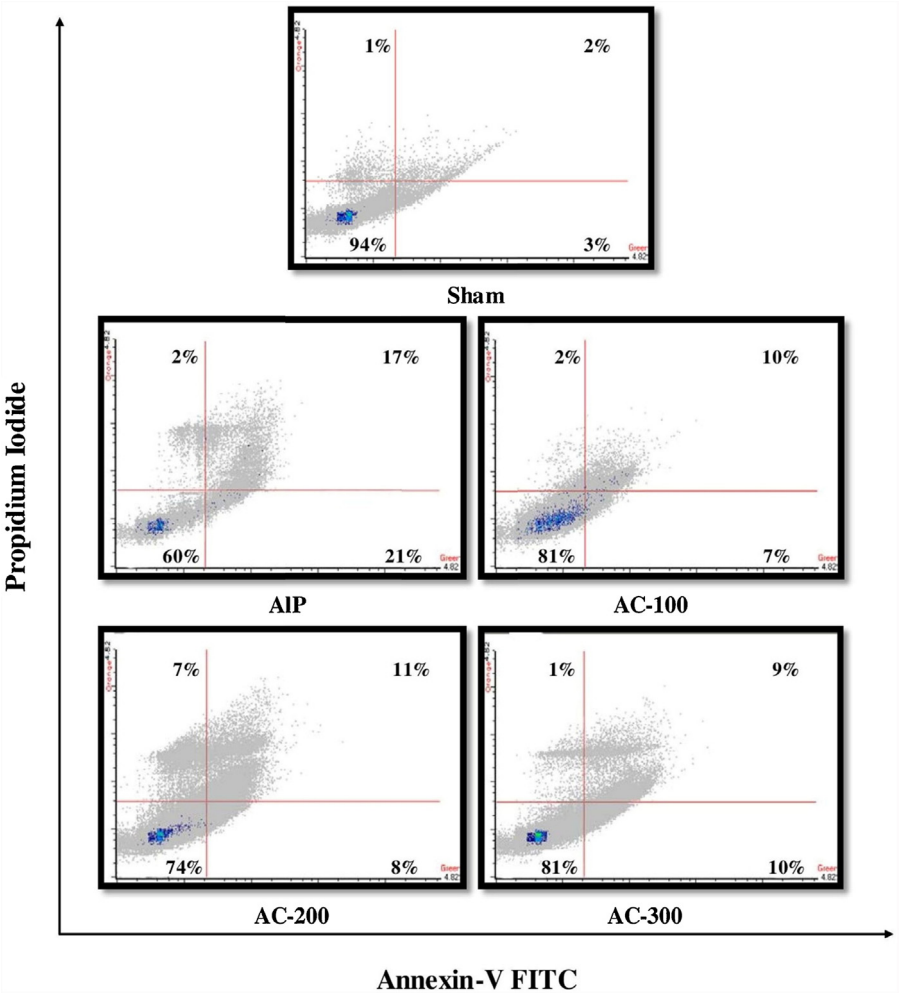


**Fig. 3.** Flow cytometry assay of apoptosis and necrosis. Each square presents the percentage of cells for annexin $V^-/PI^-$: viable cells (the number in left lower quadrant); annexin $V^+/PI^-$: early apoptotic cells (the number in right lower quadrant); annexin $V^+/PI^+$: late apoptotic cells (the number in right upper quadrant); and $V^-/PI^+$: necrotic cells (the number in left upper quadrant). Plots are representative of the results in five different experiments.

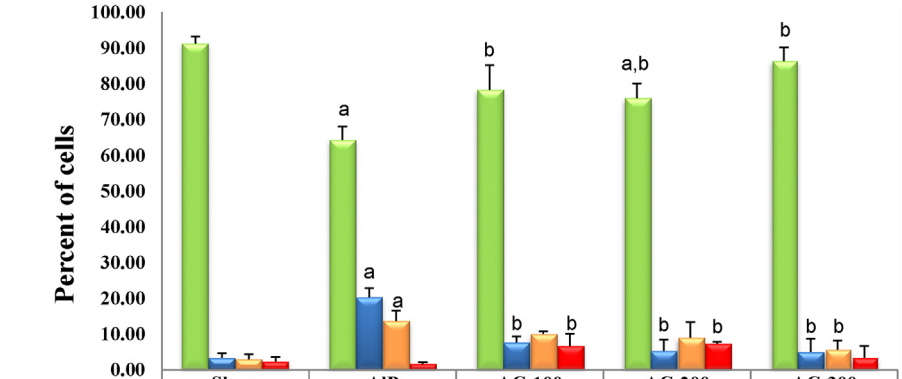


| | Sham | AlP | AC-100 | AC-200 | AC-300 |
|---|---|---|---|---|---|
| Live | 91.33 | 64.33 | 78.33 | 76.00 | 86.33 |
| Early apoptotic | 3.33 | 20.33 | 7.67 | 5.33 | 5.00 |
| Late apoptotic | 3.00 | 13.67 | 10.00 | 9.00 | 5.67 |
| Necrotic | 2.33 | 1.67 | 6.67 | 7.33 | 3.33 |

**Fig. 4.** Percentage of viable/apoptotic/necrotic cells from the flow cytometry assay. Values are mean ± SEM. [a]$P < 0.05$ vs the Sham group; [b]$P < 0.05$ vs the AlP group. Sham: no interventions; AlP: aluminum phosphide at dose of $LD_{50}$; AC-100: acetyl-L-carnitine at dose of 100 mg/kg; AC-200: acetyl-L-carnitine at dose of 200 mg/kg; AC-300: acetyl-L-carnitine at dose of 300 mg/kg.

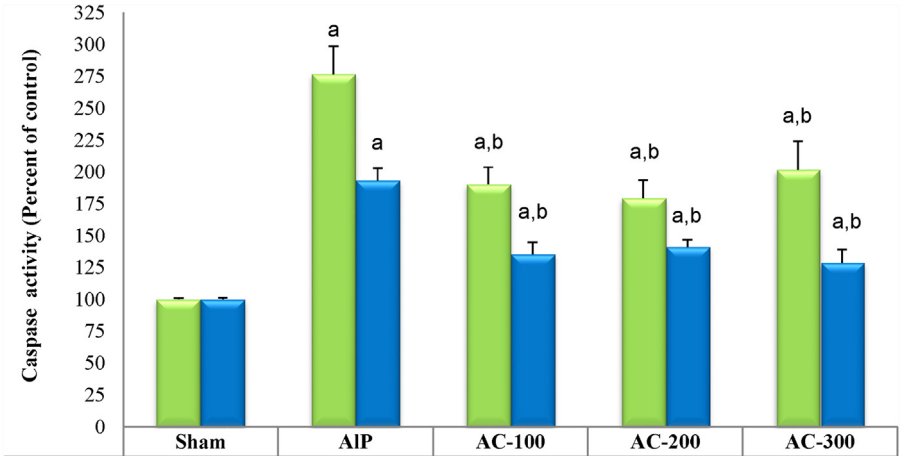


| | Sham | AlP | AC-100 | AC-200 | AC-300 |
|---|---|---|---|---|---|
| Caspase-3 | 100 | 276.63 | 190.35 | 179.28 | 201.78 |
| Caspase-9 | 100 | 193.28 | 135.28 | 141.09 | 128.64 |

**Fig. 5.** Effect of treatments on activation of caspases. Values are mean ± SEM. [a]$P < 0.05$ vs the Sham group; [b]$P < 0.05$ vs the AlP group. Sham: no interventions; AlP: aluminum phosphide at dose of $LD_{50}$; AC-100: acetyl-L-carnitine at dose of 100 mg/kg; AC-200: acetyl-L-carnitine at dose of 200 mg/kg; AC-300: acetyl-L-carnitine at dose of 300 mg/kg.

raised as compared to that of Sham ($P < 0.01$). Necrotic population were comparable between Sham, AlP, and AC-300 ($P > 0.05$), while AC-100 and AC-200 showed significant elevated values as compared to Sham and AlP ($P < 0.05$). All ALCAR groups showed notable decrease in early apoptosis compared to AlP ($P < 0.005$). However, AC-100 and AC-200 showed higher necrotic cells as compared to both Sham and AlP ($P < 0.05$, Figs. 3 and 4).

### 3.7. Caspase-3 and caspase-9 activities

Significantly higher caspase-3 and caspase-9 levels were observed in the AlP group compared to the Sham ($P < 0.01$). All ALCAR groups showed significant lower values as compared to the AlP group ($P < 0.05$); however, notable increase was observed in all groups in comparison with the Sham ($P < 0.05$). AC-200 showed the lowest caspase-3 level between ALCAR treated groups, but the difference was not statistically significant ($P > 0.05$), whilst in the case of caspase-9, AC-300 showed lower but non-significant value ($P > 0.05$). Late apoptotic population in AC-300 group was significantly lower than the AlP group ($P < 0.05$), while the other ALCAR groups showed comparable results as compared to AlP ($P > 0.05$). The AlP group did not show a significant difference from Sham in the percent of necrotic cells ($P < 0.05$, Fig. 5).

## 4. Discussion

Returning to the results, it is now possible to state that ALCAR is able to overwhelm the diverse toxic mechanisms of AlP. Mortality rate of about 70% makes AlP of most hazardous pesticides. Cardiac toxicity is the major sign of AlP toxicity plus severe ventricular arrhythmias and refractory hypotension as main clinical causes of death (Bogle et al., 2006).

Cardiomyocytes are contractile cells that form 75% of heart tissue and are responsible for its vital role in blood circulation (Brilla et al., 1991). Mitochondria play a central role in the function of cardiomyocytes. They constitute about 30% of the total cardiomyocytes volume and provide 90% of cellular energy (Carvajal and Moreno-Sanchez, 2003). Electron transport chain (ETC) which is located in the inner membrane of mitochondria is the generator of ATP for cardiomyocytes contractile function. Inhibition

of mitochondrial respiration via blockage of ETC leads to ATP depletion (King and Bailey, 2010). Phosphine is strong inhibitor of ETC. In vitro studies demonstrated that mitochondrial complex IV (cytochrome-c oxidase) is the main target of phosphine (Nath et al., 2011). The inhibition occurs through reduction of $Fe^{3+}$ in the heme structure of cytochrome-a, diminishing the electron-accepting property, and the consequent interruption of ATP production. Studies report a 45% decrease in mitochondrial complex IV, whereas there are controversial reports from no inhibition to 49% inhibition about complexes I and II (Dua and Gill, 2004; Singh et al., 2006). Several reports have shown the ability of ALCAR to increase the activity and expression of complex IV in cardiomyocytes and hepatocytes of rat (Mawal et al., 1998; Paradies et al., 1992). According to the results of our study, phosphine caused near 50% decline in complex IV activity while no inhibition was observed in complex I and II. One interesting finding is return of complex IV activity to the normal state by administration of ALCAR. These findings are consistent with prior studies (Singh et al., 2006). Moreover, inhibition of ETC by phosphine turned the normal cellular ADP/ATP ratio of 0.35–1.46 that indicates the depletion of ATP pool. As expected, ALCAR at all doses was capable of restoring cellular ATP content.

One consequence of ETC inhibition is oxidative stress caused by generation of ROS from the transport of ETC electrons to molecular oxygen and the formation of superoxide anion ($O_2^-$) (Mehrpour et al., 2014). In normal condition, this radical has a short life and mitochondrial superoxide dismutase (SOD) rapidly converts it to hydrogen peroxide ($H_2O_2$). Hydrogen peroxide is also eliminated by catalase (CAT) and glutathione peroxidase (GPx). Otherwise, it can attack cellular macromolecules and lead to cell death. Phosphine poisoning can lead to excessive ROS generation through two parallel mechanisms. The first is overproduction of ROS by disruption of the electron pathway in ETC. The latter mechanism is the alteration of antioxidant enzyme activity. Several studies have linked phosphine toxicity to increase in SOD instead of decreasing CAT and GPx activity. As pointed out in several studies, ALCAR could reduce SOD activity (reduction in $O_2^-$) and simultaneously increase the activity of CAT (increasing elimination of $H_2O_2$) (Gulcin, 2006; Loots et al., 2004).

The other mechanism considered to play a part in phosphine-induced oxidative stress is rise of free plasma iron (Cha'on et al., 2007). Due to extreme toxicity, cellular free iron level is always controlled and maintained about $10^{-18}$ M for $Fe^{3+}$ and $10^{-8}$ M for $Fe^{2+}$. Ferritin, a protein complex composed of 24 subunits, keeps the balance between soluble and insoluble ferrihydrite iron (Harrison and Arosio, 1996). It has been proved that insoluble $Fe^{3+}$ can be reduced and released from ferritin by the act of strong reducing agents ($PH_3$, for instance). The soluble $Fe^{2+}$ can generate ROS via Fenton and Haber–Weiss reactions (Cha'on et al., 2007). Gulcin has shown that ALCAR, owing to its hydroxyl and carboxyl groups, can scavenge $Fe^{2+}$ and hinder the ROS forming reactions (Gulcin, 2006). In this study, ALCAR successfully diminished elevated level of AlP induced ROS by three following actions: increasing the activity (and expression, probably) of cytochrome-c oxidase, enhancement of CAT activity, and at last, reduction in free plasma iron by its chelating property.

There are clear evidences that overproduction of ROS can lead to apoptosis acting as a second messenger. Studies have shown that ROS induced apoptosis can be mediated by both extrinsic and intrinsic pathways. In the extrinsic pathway, ROS act as death receptor activator. While in the intrinsic (mitochondrial) pathway, ROS induced mitochondrial DNA damage stimulates outer membrane permeabilization and translocation of cytochrome c to cytosol, activation of initiator caspase-9 that cleaves and activates effector caspases 3 and 7 (Solgi et al., 2015). Hence, to confirm the occurrence of apoptosis, we investigated active caspase-3 and to determine the contribution of intrinsic pathway, we examined the active caspase-9. ALCAR has been found to prevent apoptosis in several studies. Pillich et al. demonstrated the ability of ALCAR to prevent cytochrome c induced apoptosis along with stimulation of cell proliferation in cultured mouse fibroblasts (Pillich et al., 2005). Further studies on yeast and DT40 cells showed similar beneficial effects (Palermo et al., 2010; Zhu et al., 2008).

The results of flow cytometry assay show significant rise in early and late apoptotic cell population in AlP treated rats. On the other hand, concurrent ALCAR treatment prohibited phosphine induced apoptosis. One unanticipated finding was that in AC-100 and AC-200 the necrotic fractions were significantly raised compared to AlP. It is considered that the inhibition of AlP induced apoptosis by ALCAR along with elevated cellular ROS led to massive damage to cellular structures and necrosis.

The results of caspase-3 and caspase-9 assays seem to be consistent with other research which found ROS induced apoptosis is primarily conducted through the mitochondrial pathway (Jafari et al., 2015; Solgi et al., 2015). However, according to the extent of rise in active caspases against the control, it is concluded that extrinsic pathway participates in ROS induced apoptosis as well.

## 5. Conclusion

As a final point, it has been concluded that ALCAR has promising therapeutic effects of AlP poisoning by suppressing the pathways leading to oxidative stress and cell injury. From the hopeful results of this study, in addition to a long history of safety with the ALCAR, it would be interesting to assess the potential therapeutic role of it in the clinical settings of AlP poisoning.

## Conflict of interest statement

The authors declare that do not have any commercial or associative interest that represents a conflict of interest in connection with the work submitted.

## Transparency document

The Transparency document associated with this article can be found in the online version.

## Acknowledgements

This study was partially supported by a grant from TUMS coded 91-03-33-19006. The authors thank Iran National Science Foundation.

## References

Abdolghaffari, A.H., Baghaei, A., Solgi, R., Gooshe, M., Baeeri, M., Navaei-Nigjeh, M., Hassani, S., Jafari, A., Rezayat, S.M., Dehpour, A.R., Mehr, S.E., Abdollahi, M., 2015. Molecular and biochemical evidences on the protective effects of triiodothyronine against phosphine-induced cardiac and mitochondrial toxicity. Life Sci. 139, 30–39.

Anand, R., Binukumar, B.K., Gill, K.D., 2011. Aluminum phosphide poisoning: an unsolved riddle. J. Appl. Toxicol. 31, 499–505.

Baeeri, M., Shariatpanahi, M., Baghaei, A., Ghasemi-Niri, S.F., Mohammadi, H., Mohammadirad, A., Hassani, S., Bayrami, Z., Hosseini, A., Rezayat, S.M., Abdollahi, M., 2013. On the benefit of magnetic magnesium nanocarrier in cardiovascular toxicity of aluminum phosphide. Toxicol. Ind. Health 29, 126–135.

Baghaei, A., Hajimohammadi, N., Baeeri, M., Mohammadirad, A., Hassani, S., Abdollahi, M., 2014. On the protection of AlP cardiovascular toxicity by a novel mixed herbal medicine; role of oxidative stress and cellular ATP. Asian J. Anim. Vet. Adv. 9, 302–311.

Bogle, R.G., Theron, P., Brooks, P., Dargan, P.I., Redhead, J., 2006. Aluminium phosphide poisoning. Emerg. Med. J. 23, e3.

Brilla, C.G., Janicki, J.S., Weber, K.T., 1991. Impaired diastolic function and coronary reserve in genetic hypertension. Role of interstitial fibrosis and medial thickening of intramyocardial coronary arteries. Circ. Res. 69, 107–115.

Brubacher, J.L., Bols, N.C., 2001. Chemically de-acetylated 2′,7′-dichlorodihydrofluorescein diacetate as a probe of respiratory burst activity in mononuclear phagocytes. J. Immunol. Methods 251, 81–91.
Carvajal, K., Moreno-Sanchez, R., 2003. Heart metabolic disturbances in cardiovascular diseases. Arch. Med. Res. 34, 89–99.
Cha'on, U., Valmas, N., Collins, P.J., Reilly, P.E., Hammock, B.D., Ebert, P.R., 2007. Disruption of iron homeostasis increases phosphine toxicity in *Caenorhabditis elegans*. Toxicol. Sci. 96, 194–201.
Cha, Y.S., Sachan, D.S., 1995. Acetylcarnitine-mediated inhibition of ethanol oxidation in hepatocytes. Alcohol 12, 289–294.
Cui, J., Das, D.K., Bertelli, A., Tosaki, A., 2003. Effects of L-carnitine and its derivatives on postischemic cardiac function, ventricular fibrillation and necrotic and apoptotic cardiomyocyte death in isolated rat hearts. Mol. Cell. Biochem. 254, 227–234.
Dua, R., Gill, K.D., 2004. Effect of aluminium phosphide exposure on kinetic properties of cytochrome oxidase and mitochondrial energy metabolism in rat brain. Biochim. Biophys. Acta 1674, 4–11.
Duenas, A., Perez-Castrillon, J.L., Cobos, M.A., Herreros, V., 1999. Treatment of the cardiovascular manifestations of phosphine poisoning with trimetazidine, a new antiischemic drug. Am. J. Emerg. Med. 17, 219–220.
Gulcin, I., 2006. Antioxidant and antiradical activities of L-carnitine. Life Sci. 78, 803–811.
Harrison, P.M., Arosio, P., 1996. The ferritins: molecular properties, iron storage function and cellular regulation. Biochim. Biophys. Acta 1275, 161–203.
Jafari, A., Baghaei, A., Solgi, R., Baeeri, M., Chamanara, M., Hassani, S., Gholami, M., Ostad, S.N., Sharifzadeh, M., Abdollahi, M., 2015. An electrocardiographic, molecular and biochemical approach to explore the cardioprotective effect of vasopressin and milrinone against phosphide toxicity in rats. Food Chem. Toxicol. 80, 182–192.
Janssen, A.J., Trijbels, F.J., Sengers, R.C., Smeitink, J.A., van den Heuvel, L.P., Wintjes, L.T., Stoltenborg-Hogenkamp, B.J., Rodenburg, R.J., 2007. Spectrophotometric assay for complex I of the respiratory chain in tissue samples and cultured fibroblasts. Clin. Chem. 53, 729–734.
Jia, R., Bao, Y.H., Zhang, Y., Ji, C., Zhao, L.H., Zhang, J.Y., Gao, C.Q., Ma, Q.G., 2014. Effects of dietary alpha-lipoic acid, acetyl-L-carnitine, and sex on antioxidative ability, energy, and lipid metabolism in broilers. Poult. Sci. 93, 2809–2817.
King, A.L., Bailey, S.M., 2010. Assessment of mitochondrial dysfunction arising from treatment with hepatotoxicants. Curr. Protoc. Toxicol., Chapter 14, Unit14.8.
Loots, D.T., Mienie, L.J., Bergh, J.J., Van der Schyf, C.J., 2004. Acetyl-L-carnitine prevents total body hydroxyl free radical and uric acid production induced by 1-methyl-4-phenyl-1,2,3,6-tetrahydropyridine (MPTP) in the rat. Life Sci. 75, 1243–1253.
Mawal, Y.R., Rama Rao, K.V., Qureshi, I.A., 1998. Restoration of hepatic cytochrome c oxidase activity and expression with acetyl-L-carnitine treatment in spf mice with an ornithine transcarbamylase deficiency. Biochem. Pharmacol. 55, 1853–1860.
Mehrpour, O., Abdollahi, M., Sharifi, M.D., 2014. Oxidative stress and hyperglycemia in aluminum phosphide poisoning. J. Res. Med. Sci. 19, 196.
Mehrpour, O., Jafarzadeh, M., Abdollahi, M., 2012. A systematic review of aluminium phosphide poisoning. Arh. Hig. Rada Toksikol. 63, 61–73.
Minami, M., Yoshikawa, H., 1979. A simplified assay method of superoxide dismutase activity for clinical use. Clin. Chim. Acta 92, 337–342.
Nath, N.S., Bhattacharya, I., Tuck, A.G., Schlipalius, D.I., Ebert, P.R., 2011. Mechanisms of phosphine toxicity. J. Toxicol. 2011, 494168.
Nilsson, U.A., Bassen, M., Savman, K., Kjellmer, I., 2002. A simple and rapid method for the determination of "free" iron in biological fluids. Free Radic. Res. 36, 677–684.
Palermo, V., Falcone, C., Calvani, M., Mazzoni, C., 2010. Acetyl-L-carnitine protects yeast cells from apoptosis and aging and inhibits mitochondrial fission. Aging Cell 9, 570–579.
Paradies, G., Ruggiero, F.M., Gadaleta, M.N., Quagliariello, E., 1992. The effect of aging and acetyl-L-carnitine on the activity of the phosphate carrier and on the phospholipid composition in rat heart mitochondria. Biochim. Biophys. Acta 1103, 324–326.
Patel, S.P., Sullivan, P.G., Lyttle, T.S., Magnuson, D.S., Rabchevsky, A.G., 2012. Acetyl-L-carnitine treatment following spinal cord injury improves mitochondrial function correlated with remarkable tissue sparing and functional recovery. Neuroscience 210, 296–307.
Pillich, R.T., Scarsella, G., Risuleo, G., 2005. Reduction of apoptosis through the mitochondrial pathway by the administration of acetyl-L-carnitine to mouse fibroblasts in culture. Exp. Cell Res. 306, 1–8.
Schluter, K.D., Schreiber, D., 2005. Adult ventricular cardiomyocytes: isolation and culture. Methods Mol. Biol. 290, 305–314.
Singh, S., Bhalla, A., Verma, S.K., Kaur, A., Gill, K., 2006. Cytochrome-c oxidase inhibition in 26 aluminum phosphide poisoned patients. Clin. Toxicol. 44, 155–158.
Siwach, S.B., Singh, H., Jagdish, Katyal, V.K., Bhardwaj, G., 1998. Cardiac arrhythmias in aluminium phosphide poisoning studied by on continuous holter and cardioscopic monitoring. J. Assoc. Physicians India 46, 598–601.
Slaughter, M.R., O'Brien, P.J., 2000. Fully-automated spectrophotometric method for measurement of antioxidant activity of catalase. Clin. Biochem. 33, 525–534.
Smith, L., 1955. Spectrophotometric assay of cytochrome c oxidase. Methods Biochem. Anal. 2, 427–434.
Solgi, R., Baghaei, A., Golaghaei, A., Hasani, S., Baeeri, M., Navaei, M., Ostad, S.N., Hosseini, R., Abdollahi, M., 2015. Electrophysiological and molecular mechanisms of protection by iron sucrose against phosphine-induced cardiotoxicity: a time course study. Toxicol. Mech. Methods 25, 249–257.
Tompkins, A.J., Burwell, L.S., Digerness, S.B., Zaragoza, C., Holman, W.L., Brookes, P.S., 2006. Mitochondrial dysfunction in cardiac ischemia-reperfusion injury: ROS from complex I, without inhibition. Biochim. Biophys. Acta 1762, 223–231.
Zhu, X., Sato, E.F., Wang, Y., Nakamura, H., Yodoi, J., Inoue, M., 2008. Acetyl-L-carnitine suppresses apoptosis of thioredoxin 2-deficient DT40 cells. Arch. Biochem. Biophys. 478, 154–160.